A ROTATING FLUX COMPRESSOR FOR ENERGY CONVERSION*

P. Chowdhuri, T. W. Linton and J. A. Phillips
Los Alamos National Laboratory
Los Alamos, New Mexico 87545

Summary

The rotating flux compressor (RFC) converts rotational kinetic energy into an electrical output pulse which would have higher energy than the electrical energy initially stored in the compressor. An RFC has been designed in which wedge-shaped rotor blades pass through the air gaps between successive turns of a solenoid, the stator. Magnetic flux is generated by pulsing the stator solenoids when the inductance is a maximum, i.e., when the flux fills the stator-solenoid volume. Connecting the solenoid across a load conserves the flux which is compressed within the small volume surrounding the stator periphery when the rotor blades cut into the free space between the stator plates, creating a minimum-inductance condition. The unique features of this design are: (1) no electrical connections (brushes) to the rotor; (2) no conventional windings; and (3) no maintenance. The device has been tested up to 5,000 rpm of rotor speed.

Introduction

The rotating flux compressor (RFC) converts rotational kinetic energy into an electrical output pulse which would have higher energy than the electrical energy initially stored in the compressor.

The principle of the flux compressor can be explained by Fig. 1. The flux compressor is a variable inductor, where the inductance is varied by external means. It is charged from a current source when it has its maximum inductance L_{max}. The current source is disconnected at the end of the charging period, and the inductance of the flux compressor is forced towards its minimum value L_{min}. The load L_ℓ is also connected to the flux compressor at the same time. Because of the conservation of flux linkage, the load current increases, if $L_{max} >> L_\ell$. Thus,

$$I_i \cdot L_{max} = I_f \cdot (L_{min} + L_\ell) \tag{1}$$

or,

$$I_f/I_i = \frac{L_{max}}{L_{min} + L_\ell} \tag{2}$$

Similarly,

$$U_i = (1/2) \cdot I_i^2 L_{max} \tag{3}$$

$$U_f = (1/2) \cdot I_f^2 (L_{min} + L_\ell) \tag{4}$$

and,

$$U_f/U_i = (I_f/I_i)^2 \cdot \frac{L_{min} + L_\ell}{L_{max}} = \frac{L_{max}}{L_{min} + L_\ell} \tag{5}$$

Both the final current and the final energy can be many times their initial values if $L_{max} >> (L_{min} + L_\ell)$. In a rotating flux compressor, the increase in the final energy is accomplished at the expense of the kinetic energy of the rotors, i.e., by slowing the rotor speed.

The mechanism by which the inductance of a flux compressor is varied can be explained by Figs. 2 and 3. In Fig. 2a, a solenoid is charged from a current source while a cylinder of high electrical conductivity is moving towards the air core inside the solenoid. In Fig. 2b, the current source is disconnected and the load L_ℓ is connected, when the conducting cylinder is about to enter the solenoid core. Figure 2c shows the condition at the end of the cycle. As the conducting cylinder moves into the solenoid core it displaces the core magnetic flux and squeezes it around the solenoid turns. This effectively reduces the solenoid inductance. Hence, the solenoid inductance is L_{max} in Fig. 2a, while it is L_{min} in Fig. 2c.

In the rotating flux compressor, the conducting cylinder of Fig. 2 becomes the rotor and the solenoid the stator (Fig. 3a). When the stator solenoid (Fig. 3b) is energized, the magnetic field lines fill the central region. Under this condition, the solenoid has the maximum inductance L_{max}. The rotors, consisting of a number of parallel plates, pass between the windings, Fig. 3c. Magnetic field lines are cut, reform about the windings, and the magnetic energy which filled the solenoid is now compressed between the plates and the sides of the windings (Fig. 3d). A large decrease in volume (inductance) takes place. Figure 4 shows the cross-section of a two-solenoid rotating flux compressor when the wedge-shaped rotor passes over the central air core of each solenoid. The hatched parts represent the compressed magnetic flux.

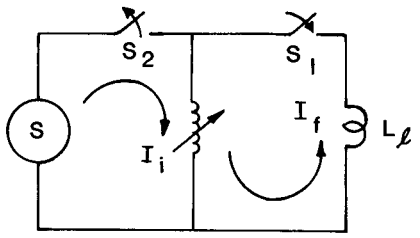

Fig. 1. Schematic for flux-compression test.

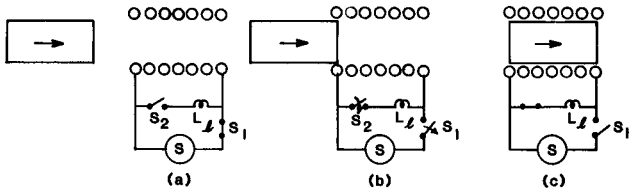

Fig. 2. Flux compression by a moving metallic cylinder.

*Work performed under the auspices of the US Dept. of Energy.

Report Documentation Page

Form Approved
OMB No. 0704-0188

1. REPORT DATE	2. REPORT TYPE	3. DATES COVERED
JUN 1983	**N/A**	**-**

4. TITLE AND SUBTITLE	5a. CONTRACT NUMBER
A Rotating Flux Compressor For Energy Conversion	5b. GRANT NUMBER
	5c. PROGRAM ELEMENT NUMBER
6. AUTHOR(S)	5d. PROJECT NUMBER
	5e. TASK NUMBER
	5f. WORK UNIT NUMBER
7. PERFORMING ORGANIZATION NAME(S) AND ADDRESS(ES) **Los Alamos National Laboratory Los Alamos, New Mexico 87545**	8. PERFORMING ORGANIZATION REPORT NUMBER
9. SPONSORING/MONITORING AGENCY NAME(S) AND ADDRESS(ES)	10. SPONSOR/MONITOR'S ACRONYM(S)
	11. SPONSOR/MONITOR'S REPORT NUMBER(S)

12. DISTRIBUTION/AVAILABILITY STATEMENT
Approved for public release, distribution unlimited

13. SUPPLEMENTARY NOTES
See also ADM002371. 2013 IEEE Pulsed Power Conference, Digest of Technical Papers 1976-2013, and Abstracts of the 2013 IEEE International Conference on Plasma Science. Held in San Francisco, CA on 16-21 June 2013. U.S. Government or Federal Purpose Rights License.

14. ABSTRACT

15. SUBJECT TERMS

16. SECURITY CLASSIFICATION OF:			17. LIMITATION OF ABSTRACT	18. NUMBER OF PAGES	19a. NAME OF RESPONSIBLE PERSON
a. REPORT	b. ABSTRACT	c. THIS PAGE			
unclassified	**unclassified**	**unclassified**	**SAR**	**4**	

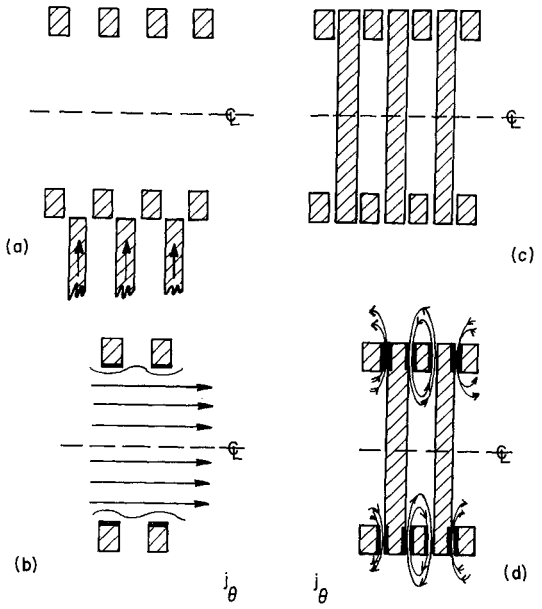

Fig. 3. Mechanism of flux compression by rotating conducting disks.

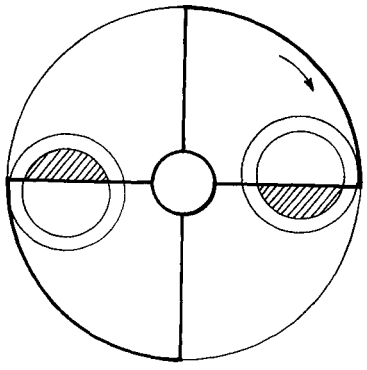

Fig. 4. Cross-section of a two-solenoid rotating flux compressor and its wedge-shaped rotor.

Los Alamos Design of Rotating Flux Compressor

The present RFC model consists of 16 aluminum stator plates and 15 aluminum rotor blades, each 0.95 cm thick, as shown in Fig. 5. The stator plates are connected such that they form two pairs of 16-turn solenoids. The rotor blades rotate in the 1.15 cm wide air gaps between the successive stator plates. The outside diameter of a stator plate is 55.25 cm. The stator cores are tear-drop shaped to produce relatively high rate of rise of the output current near the minimum inductance. The rotor blades are rotated by an air turbine.

The unique features of this design include:

1. no electrical connections (brushes) to the rotor i.e., switches that initiate the output electrical pulse are located outside the generator;

2. the device is sturdy because there are no conventional windings either on the rotor or on the stator; and

3. the device is maintenance-free.

A photograph of the complete assembly is shown in Fig. 6.

Tests on the RFC

The circuit for testing the RFC is similar to Fig. 1. The current source is four banks of 70-mF electrolytic capacitors charged to variable voltages. Initially S_2 is closed and S_1 is open. The RFC is brought to the required speed, and the capacitor banks are charged to the required voltage. The capacitor banks are then discharged by an ignitron (not shown) in series with S_2. The switch S_1 is closed and S_2 opened at the peak of the discharge current. The sequence of ignitron firing, operation of S_1 and S_2, and oscilloscope triggering is done by a time-delay generator which in turn is triggered by an electrical pulse generated by an opto-electronic sensor coupled to the RFC rotor. The delay time for the switch operation is varied with the rotor speed so that the peak of the capacitor-bank discharge current occurs when the rotor blades start to obstruct the stator

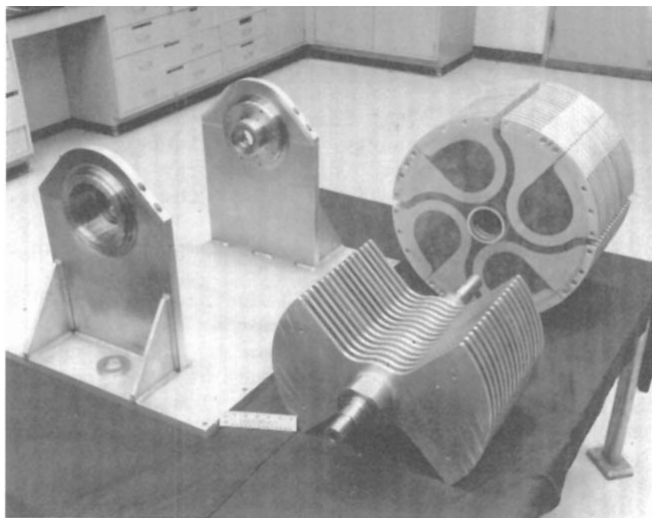

Fig. 5. Rotor blades and stator plates of the Los Alamos rotating flux compressor.

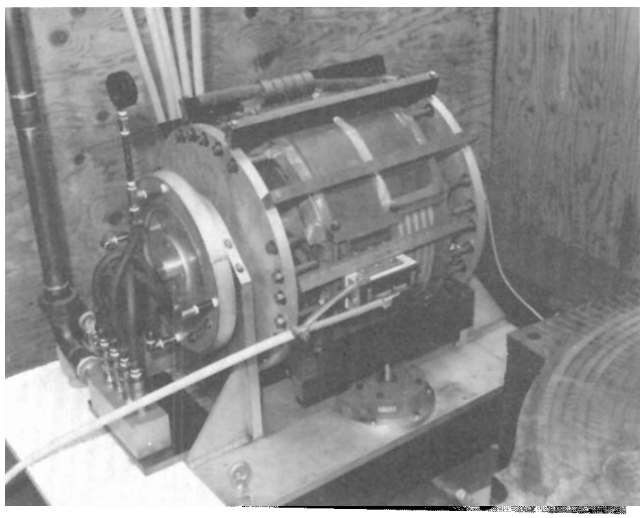

Fig. 6. Los Alamos rotating flux compressor.

cores. Tests were performed at various rotor speeds to measure current amplification. Figure 7 shows typical oscillograms of the load and input currents with one pair of 16-turn stator-solenoids in circuit.

Discussion

When the rotor blades sweep inside the free space between the stator plates, the magnetic flux is displaced and compressed around the periphery of the stator plates, decreasing the inductance of the RFC system. A smaller confinement volume of the magnetic flux results in smaller inductance. The flux compression that depends upon the $L_{max}/(L_{min} + L_\ell)$ ratio will thus be larger the smaller the L_{min} for specified L_{max} and L_ℓ. The magnetic flux, however, is not entirely confined within the free space between the stator plates and the rotor blades. The flux diffuses into the rotor and the stator materials. As the magnetic flux diffuses into these materials, the effective volume of flux confinement increases, thus increasing L_{min} and degrading flux compression.

If a conducting plate is exposed to a pulsed magnetic field, the time-domain analysis of flux diffusion through the plate can be performed starting with the one-dimensional diffusion equation. Thus,

$$d^2H/dx^2 = (\sigma\mu)(dH/dt) \quad , \tag{6}$$

where H = magnetic field,
σ = electrical conductivity of the conducting plate,
μ = permeability of the conducting plate,
x = depth within the plate from its surface, and
t = time.

Assuming a step-function magnetic field, i.e.,

$$H_u(0,t) = H_o u(t) \quad , \tag{7a}$$

and,

$$\lim_{x\to\infty} H_u(x,t) = 0 \quad , \tag{7b}$$

the solution becomes

$$H_u(x,t) = H_o \mathrm{erfc}[(x/2)\sqrt{(\sigma\mu/t)}] \quad . \tag{8}$$

This is the solution for the magnetic field diffusing inside a conducting plate by an applied step-function magnetic field. The solution for any other type of time-varying magnetic field is obtained by applying the convolution integral.

Equation (8) shows that the depth of flux penetration will be less for highly conductive materials. It also shows how the flux penetrates the conducting plate as a function of time. Translating this to the rotating flux compressor, the flux penetration will be smaller the faster the rotor blades sweep pass the stator cores. In other words, the higher the rotor speed the higher will be the L_{max}/L_{min} ratio, and consequently the higher will be the current amplification. Figure 8 shows the measured variation of the current amplification as a function of the rotor speed.

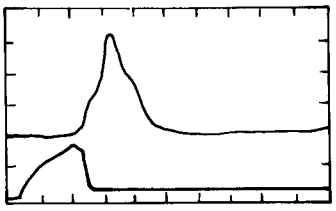

Fig. 7. Output and input current profiles of the rotating flux compressor.
Rotor speed = 5000 r.p.m.
Load inductance L_ℓ = 0.02 μH.
Upper trace: Output current, 2kA/div; 1 ms/div.
Lower trace: Input current, 1.08 kA/div; 1 ms/div.
One pair of 16-turn stator-solenoids in circuit.

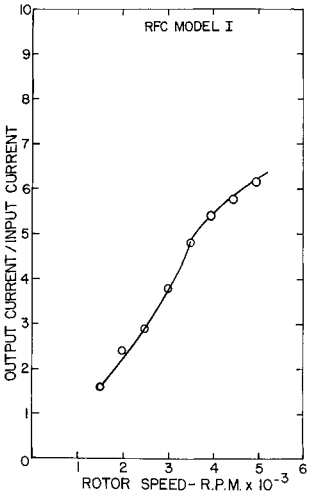

Fig. 8. Current amplification vs. rotor speed. L_ℓ = 0.02 μH. One pair of 16-turn stator-solenoids in circuit.

The L_{max} condition occurs when the magnetic flux flows through the stator cores unobstructed by the rotor blades. The L_{max} can be significantly improved, and so will the current amplification, if the stator cores are filled with a ferromagnetic material and the rotor blades are also partially built with the ferromagnetic material. We have initiated work on a ferromagnetic RFC.

The inductance and resistance of the RFC were measured with an impedance bridge at three frequencies for various rotor positions (Fig. 9). One pair of 16-turn stator-solenoids was in circuit. The L_{max} is the highest (29 μH) at 120 Hz and the lowest (23.3 μH) at 10 kHz. At high frequencies, the excitation current tends to flow along the innermost periphery of the stator coils surrounding the central air core. As the magnetic flux is confined within a smaller volume under this condition, the L_{max} is also smaller. The L_{min}, likewise, is the highest (5 μH) at 120 Hz and the lowest (1.9 μH) at 10 kHz. During flux compression, the magnetic flux diffuses into the surrounding metals, penetrating further into the metals for lower frequencies. Thus, for lower frequencies, the volume of the confined magnetic flux will be larger, and hence the L_{min} higher.

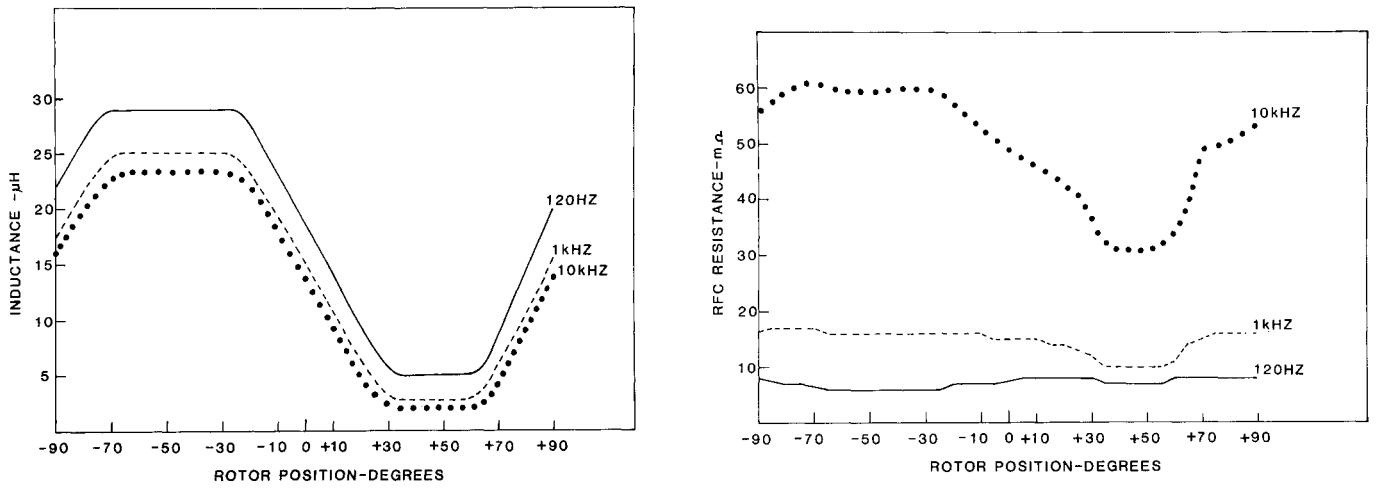

Fig. 9. RFC impedance as a function of rotor position, measured with an impedance bridge. One pair of 16-turn stator-solenoids in circuit. (a) inductance; (b) resistance.

The calculated value of L_{max} for the 32-turn stator, assuming uniform current distribution, is 33.2 μH, and that of a single turn 0.25 μH.

The variation of the RFC resistance with rotor position is small at 120 Hz, but pronounced at 10 kHz (Fig. 9b).

The RFC resistance has three components:

1. bulk resistance of the stator coils,
2. contact resistance between stator coils, and
3. effective resistance of the eddy-current losses during flux diffusion.

As mentioned earlier, the excitation current tends to flow along the innermost periphery of the stator coils surrounding the central air core during the period of L_{max}, i.e., when the rotor blades are not obstructing the central air cores of the stators. Higher the excitation-current frequency the smaller the cross-section of current flow, and hence higher the bulk resistance. Magnetic flux is deflected as the rotor blades start to obstruct the stator core. This redistributes the stator current, forcing it to flow over a larger cross-section, thus reducing the bulk resistance to current flow. However, flux diffusion generates eddy-current losses, introducing more resistance. The total resistance rises during flux compression at 120 Hz, indicating that the effective resistance of the eddy-current losses is predominant. However, at 1 kHz and 10 kHz, the total resistance drops during flux compression, indicating that the decrease of the bulk resistance is more pronounced than the increase caused by the eddy-current losses.

The calculated dc resistance of the RFC is 2.4 mΩ, compared to the measured dc resistance of 3.4 mΩ. The difference is caused by the contact resistance between the 32 turns of the stator.

The switches S_1 and S_2 of Fig. 1 are stationary fast-acting multiple-contact switches installed external to the RFC. The opening switch S_2 is immersed in pressurized hydrogen to minimize arcing and hence erosion. In recent experiments, we have replaced the closing switch S_1 with a silicon rectifier. This prevents reverse current to flow through the load, enables faster transfer of current to the load and shortens arc interruption time of S_2 even further. We plan to replace S_2 eventually by solid-state switches.

Conclusions

We have performed magnetic flux compression with a rotating flux compressor of simple design which does not need brushes or sliding contacts, and which does not have conventional windings either on the rotor or on the stator. Flux compression was achieved with current amplification increasing with rotor speed to 6.4 at 5,000 rpm.

Acknowledgements

The authors acknowledge the contributions of many of their colleagues, particularly to G. A. Barnes, J. G. Garcia and K. H. Milder for help with the tests; and to A. R. Wilson, Jr. for the original RFC construction.